THE EFFECT OF MICROSTRUCTURE ON THE CLEAVAGE STRENGTH OF QUENCHED AND TEMPERED STEELS

to

N A S A

Contract No. NSG-622

SU-DMS-68-R-102

A. S. Tetelman
Associate Professor
Department of Materials Science
Stanford University
Stanford, California

The effect of microstructure on the cleavage strength of quenched and tempered steels

D.E. Hodgson*, Ph.D. and Prof. A.S. Tetelman,+ Ph.D.
Dept. of Materials Science, Stanford University, Stanford, California USA
*Now at Battelle Memorial Institute, Columbus, Ohio
+Now at Materials Division, School of Engineering, UCLA, Los Angeles, Calif. USA

Abstract A series of carbon-maganese steels, containing 0.18 to 0.81% carbon and 0 to 1.5% manganese were austenitized, quenched, and tempered. These compositions and heat treatments allowed a variation of maximum carbide size from 0.2 to 5 microns and a variation of free interparticle spacing from 0.13 to 3.0 microns.

Standard Charpy V-notch specimens were fractured in slow threepoint bending over a range of temperatures from -196C to -75C where fracture occurred by cleavage. Companion tensile tests were conducted over the same temperature range to determine the effect of microstructure on the tensile yield strength, σ_Y. The critical tensile stress required to cause cleavage fracture below the notch root, σ_f^*, was computed by elastic-plastic analyses, wherein $\sigma_f^* = 2.18\ \sigma_Y$ at the point where $P_F = 0.8\ P_{GY}$. P_F is the notched fracture load and P_{GY} the (extrapolated) value of the general yield load.

The values of σ_f^* varied from 159 to 370 ksi as the microstructure was refined. These values were quantitatively compared with theoretical values for single phase and dispersed systems. The data indicate that in fine microstructures σ_f^* is determined primarily by the free interparticle spacing. In coarse microstructures, particles may act as Griffith-type flaws if the free ferrite path length is sufficient to permit pile-ups to crack the particles; σ_f^* is then determined by the maximum size of the carbide particles. The results also indicate that the presence of a few large particles may not cause a decrease in cleavage strength if the microstructure is refined by a homogeneous distribution of smaller particles.

Introduction

The effect of low volume fractions (< 15%) of hard particles on the low temperature cleavage processes in dispersed systems such as spheroidized steel has received little systematic study. From a series of isolated experiments on a variety of materials tested at temperatures where the matrix is capable of failing by cleavage, it appears that the particles can assist or inhibit the cleavage process in the following ways:

1. At small plastic strains the particles may crack or separate from the matrix, creating Griffith-type flaws which are more effective

stress concentrators for promoting matrix cleavage than are blocked slip bands (1). The cleavage strength, σ_f^*, is then reduced by the introduction of the large particles.

2. A network of thin particles at matrix grain boundaries may effectively harden the boundaries and inhibit plastic relaxation around blocked slip bands and incipient microcracks (2). The cleavage strength is then reduced by the introduction of the particles (3).

3. The particles may effectively block microcracks which have formed in the matrix, limiting their size to that of the particle spacing (4). The cleavage strength is then increased by the introduction of the particles.

4. The particles may block slip processes in the matrix, reducing the length of dislocation pile-ups which initiate fracture and thereby increase the cleavage strength of the system (5).

5. The particles may have no direct effect on the fracture process, but may increase the cleavage strength by causing the matrix grain size to be refined during heat treatment.

6. Finally, on a macroscopic scale, the particles may reduce the triaxial stress state around a notch if the particle-matrix interfaces are weak in shear, by promoting a more homogeneous deformation pattern in the vicinity of the notch (6). This reduction in triaxiality leads to an increase in macro toughness parameters such as K_{IC} and a reduction in nil-ductility temperature.

It seems certain that the effect of particles on cleavage fracture is not the same in all dispersed systems. In fact, in any one system two or more of these processes may be occurring simultaneously. This is particularly the case in commercial materials that contain more than one type of particle, or in which there exists a wide distribution of particle sizes.

The current investigation was performed to quantitatively determine the effect of particle size, spacing and volume fraction on the microscopic cleavage fracture strength of a system containing low volume fractions of hard, spherical particles which are strongly bonded to the matrix but which are not coherent with it. It was determined that for the spheroidized carbon-manganese steel investigated here, the predominant effects of particles on cleavage fracture are those described above as effects (1) and (4).

Experimental Procedure

A series of carbon and carbon-manganese steels were chosen as the subject for this investigation. The compositions are given in Table I.

TABLE I

Steel* design	Carbon (wt%)	Mn (wt%)	S (wt%)	All Others	Calc. Vol. % carbide
18MS	0.18	1.15	0.016	trace	2.74
44	0.44	0.01	0.005	"	6.95
44M	0.44	1.44	0.005	"	6.95
44MS	0.44	1.50	0.065	"	6.95
60	0.60	0.01	0.005	"	9.45
73	0.73	0.01	0.005	"	11.50
81M	0.81	0.98	0.005	"	12.73

*Note that the steel designation indicates the amount of carbon and whether the steel contains manganese or sulfur in significant amounts.

The steels were austenitized to yield an austenite grain size of ASTM No. 3 (0.1mm), quenched in oil and tempered in static vacuum at temperatures from 450 to 715C for 24 hours. Typical structures of one steel tempered at three temperatures are shown in figure 1. The microstructural parameters were measured from electron microscopy replicas of polished and electro-etched surfaces and the structures were characterized using the following formulas (7).

$$\lambda_p = \frac{1-f}{N_L} \; ; \; \bar{d} = \sqrt{\frac{3}{2}} \; \frac{\lambda_p f}{1-f} \text{ and } D_s = \frac{\bar{d}}{2}\sqrt{\frac{\pi}{f}} \qquad (1)$$

where λ_p = mean free particle spacing

N_L = number of particles per unit length of random line on the microstructure

f = volume fraction of carbide

$\bar{d}$ = calculated mean planar particle diameter

D_s = interparticle spacing (mean planar center-to-center particle spacing).

The volume fraction of the carbide measured on the micrographs was always somewhat greater than calculated from the composition (generally by about 20%) but the error was not sufficient to significantly affect the calculated microstructural parameters. The value of "f" determined from the composition was used in all calaulations for consistency. In the steels which contained more than the minimum amount of sulfur, the sulfur appeared as rather elongated MnS inclusions with a major dimension of up to 10 microns regardless of the heat treatment.

One special microstructure was prepared to determine the effect of carbide particle size distribution. In the normal structures, the particle size-frequency curve indicated a Gaussian distribution with a slight weighting toward the smaller particle sizes. This is roughly in accord with the findings of Hahn and Rosenfield (8). Preparing the special structure involved quenching and tempering steel 81M at a high temperature (700C), rapidly heating to 850C for two minutes (reaustenitizing) and then requenching and tempering at 450C. The resulting microstructure was a uniform dispersion of very fine particles containing a few large particles retained

from the original quench and temper. This structure is shown in Figure 2.

Sheet tensile specimens and slow-bend Charpy V-notch specimens of each structure were tested at temperatures from -196C to 23C. The tensile specimens furnished yield data as a function of temperature and the Charpy specimens provided the data necessary to determine the fracture properties of the materials. Two stage electron microscopy replicas were used to determine the type of fracture occurring in the Charpy specimens and to detect, if possible, the effect of the particles on the fracture process.

Experimental Results

The microstructural parameters determined for each structure are given in Table II. The values for the double-quenched-and-tempered structure are extrapolated from the higher tempering temperatures for steel 81M as the structure was too fine to accurately measure any values but d_{max}, the maximum particle size. For all other structures, the calculated values of $\bar{d}$, the mean particle size, were in good agreement with values estimated from the micrographs, leading to confidence in the numerical description of the microstructures.

The ambient temperature tensile yield strength of each microstructure is given in Table II. Even at liquid nitrogen temperature, plane tensile specimens of these steels fracture by ductile rupture, which occurs at tensile stress levels well below that required to cause cleavage. In order to study the effect of microstructure on cleavage strength it was therefore necessary to use bars of Charpy V-notch geometry in which the tensile stress level can be raised above the tensile yield strength, σ_Y by the triaxial constraint below the notch. The detailed procedure is described in reference (2), and is outlined in figure 4. Briefly, it has been shown (9) that when the applied load, P, is 0.8 of the load required for

general yielding, P_{GY}, the maximum tensile stress level, σ_{yy}, in the plastic zone ahead of the V-notch in a perfectly plastic solid is 2.18 σ_Y. This occurs at a point located in the plane of the notch, about two notch root radii ahead of the notch tip, and is the site of fracture initiation. The general yield load curve (figure 4) is extrapolated a bit below the temperature $T_{D(N)}$ (where fracture occurs upon general yield) to the temperature T* where $P_F = 0.8P_{GY}$. From companion tensile tests, the value of σ_Y is determined at T* so that the maximum stress level in the plastic zone at fracture (i.e., the fracture strength) is given by

$$\sigma_f^* = 2.18\ \sigma_Y \text{ (evaluated at T*)} \qquad (2)$$

Although this approach is strictly valid for non-strain hardening solids, it probably gives a good approximation of the effect of relative changes in microstructure on fracture strength in a given alloy system having similar strain hardening characteristics. There is abundant evidence (10, 11) to show that the values of σ_f^* determined by this type of an approach are roughly independent of temperature provided there is no change in the mode of fracture initiation, such as from twinning to slip. Since all of our fractures were slip-nucleated, the fact that σ_f^* for the various microstructures was determined at different temperatures (see Table II) is no hindrance in comparing the relative values.

The major theories of yielding and fracture in dispersed systems predict that the yield strength should vary as the reciprocal of the particle spacing or as the reciprocal square root of some "effective grain size" (12). The fracture stress should vary, if theory is obeyed, as the reciprocal square root of this same effective grain size or as the reciprocal square root of the maximum particle size (8). The yield and fracture strength values from Table II were therefore plotted against

the appropriate microstructural parameters as shown in figures 5-7. It is seen that the yield strength varies linearly with the reciprocal square root of the free interparticle spacing while the fracture strength shows a linear dependence on both $d_{max}^{-1/2}$ and $(D_s-\bar{d})^{-1/2}$ in different ranges of particle sizes.

Electron fractographs of the broken specimens showed that the fractures were almost entirely cleavage with a few very small ($< 25\ \mu$ dia.) patches of fibrous rupture near the notch root in some specimens. These patches were considered too small to have formed by slow crack growth and probably formed as the fracture propogated toward the free surface after initiating some distance below the notch in the region of high triaxial stress. The cleavage fracture surfaces were quite rough and there appeared to be many individual initiation sites. In most cases, there was little discernible interaction between the particles and the traveling cleavage crack. At the initiation points, it was sometimes possible to find a carbide particle but many of the facets seemed to initiate at no distinct point in the structure.

Discussion

A number of theories have been proposed to explain the yield behavior of dispersion-strengthened systems. In simple systems a basic mechanism such as Orowan bowing (13) often controls yielding; in more complex cases where grain boundaries and substructure are present this is not the case. Spheroidized steels are typical of this latter category. In agreement with Liu (12) and Mima (14), the results of this study show that the yield strength is a linear function of the reciprocal square root of some measure of dispersion spacing. The least scatter was found when plotting the yield strength, σ_Y, against the reciprocal square root of the free interparticle spacing, $(D_s-\bar{d})^{-1/2}$ (see figure 6).

The yield results are in accord with the conclusions of Turkalo (15) and Embury, Keh, and Fisher (16). Turkalo used transmission electron microscopy to show that dislocation cell walls, or sub-grain boundaries, exist between the particles in spheroidite. The particles thus act as "corners" to pin a sub-grain structure of the same size as the interparticle spacing. Embury et al. showed that continued cold working refined the sub-grain structure, or cell size, in rolled and drawn pearlite. They found that the flow stress varied as the reciprocal square root of this cell size. The linear relation obtained by Embury et al. is plotted in figure 6 and it is seen that their values for flow stress coincide almost exactly with the values for yield stress in the spheroidite. This indicates that the chosen measure of the "effective grain size" in spheroidite is correct and the particles are influencing yielding only as they serve to pin the dislocation substructure during the tempering treatment.

The initiation and unstable propogation of microcracks through the large carbide particles should obey the same general laws as those which describe microcrack initiation and initial propogation in a single-phase material. According to the Cottrell-Petch model, for example, the tensile stress, σ_c, required to cause cracks to spread through the carbides would be

$$\sigma_c = \frac{2\gamma_c}{nb} = \frac{G_c \gamma_c}{k} (D_s - d)^{-1/2} \qquad (3)$$

where G_c is the shear modulus of the carbides, γ_c is the work required for propogation through the carbide, n is the number of dislocations that have piled up at the carbide-matrix interface, b is the Burger's vector of the dislocations, and k is the Petch parameter that describes the variation of flow stress with $(D_s - \bar{d})^{-1/2}$ in figure 6. In plane tensile specimens, σ_c is greater than σ_Y so that large amounts of strain hardening and hence large

plastic strains would be required to develop cracks that can propogate through the large carbides. In the notched specimens employed in the present investigation, however, the local tensile stresses in the plastic zone reach 2.18 σ_Y, which probably accounts for the development of carbide cracks at small plastic strains. An example of such a crack is shown in figure 3.

If carbide cracks are, in turn, able to propogate into the ferrite and cause the observed matrix cleavage, then the cleavage strength, σ_f^*, will be given either by σ_c or by the stress required for carbide crack propogation into the matrix, σ_p, whichever is the greater. The stress σ_p is given by

$$\sigma_p = \left[\frac{E\gamma_f}{\pi(1-\nu^2)}\right]^{-1/2} d^{-1/2} \qquad (4)$$

where E is the elastic modulus, γ_f is the effective ferrite surface energy, ν is Poisson's ratio and d is the carbide particle size. The presence of non-propogating carbide cracks (figure 3) suggests that $\sigma_p > \sigma_c$ for structures containing large carbides. Furthermore, the fact that σ_f^* increases with decreasing d_{max} even when $(D_s - \bar{d})$ is maintained constant (compare steels 81M and 44, and 73 and 44MS in Table II) suggests that equation (4) rather than (3) is controlling and that $\sigma_f^* = \sigma_p$ should vary linearly with $d_{max}^{-1/2}$. As seen in figure 7, this is roughly true for those structures containing carbides larger than one micron in diameter. The value of γ_f, the work done in propogating a microcrack through the ferrite, is 5×10^4 ergs/cm^2, which is similar to that reported by Low (17) for crack propogation in ferrite.

When both large particles and a fine microstructure are present, as in the double-quenched-and-tempered structure, then σ_c can be greater than σ_p, and σ_f^* will be given by the value of σ_c, the tensile stress required to cause particle cracking. As shown in figure 7, σ_f^* for the DQT structure is

50% greater than predicted by a fracture criterion based simply on the propogation of cracks out of the large carbide particles. This is very important from a practical viewpoint because it implies that isolated large particles in a structure containing a fine dispersion may not cause appreciable decrease in cleavage strength; slip bands of sufficient size are also required to crack the particles in the first place.

Comparison of figures 6 and 7 reveals that those points which do not obey equation 2 in figure 7 fail within a fairly narrow, linear band in figure 6. In these finer structures, as well as in some overlap from the coarser structures, the fracture stress varies as the reciprocal square root of the free interparticle spacing, but does not extrapolate to zero. The basis for this type of fracture dependence was proposed by Petch in 1953 (18) and has since been studied and revised by numerous investigators (19). The slope of the fracture stress vs. (grain size)$^{-1/2}$ curve and whether or not it should extrapolate to zero stress at infinite grain size have been the object of many studies and much speculation. These points are still unresolved. The fact that the band in figure 6 includes the value of the fracture stress of a mild, high nitrogen steel studied by Wilshaw et. al. (20) leads to the conclusion, though, that the behavior of spheroidite is not at variance with that of coarser steels.

Recently, Hahn and Rosenfield (5) revised Cottrell's mechanism of double-pile-up crack initiation (21) and showed that a relatively fine dispersion can block the slip processes necessary for crack initiation and thus raise the fracture stress. Their expression, when strictly applied, does not predict the form of the fracture stress shown in figure 6. This is not surprising, as their relation is based on a different yield criterion than found in spheroidite. The major phenomenological conclusion drawn by Hahn and Rosenfield is confirmed, however, by the results in this study.

This is that as the particle spacing and size are decreased in a dispersed system, the fracture strength changes from a dependence on cracked particles as Griffith flaws to a dependence on the size of the free slip distance available to concentrate stress and initiate fracture. The point at which this change in dependence occurs cannot be defined precisely from figures 6 and 7, but seems to be at about one micron maximum particle size or interparticle spacing. This is in agreement with the predictions made by Hahn and Rosenfield (8).

Summary

A series of plain carbon spheroidized steels containing various sizes and amounts of carbide particles were tested from -196C to 23C to determine their yield and fracture properties. The major conclusions which can be drawn are:

1. The yield strength at 23C varies as the inverse square root of the planar interparticle spacing.
2. The cleavage fracture strength obeys a Griffith criterion for failure if the following conditions hold.
   a) Carbide particles approximately one micron in diameter or larger are present.
   b) The matrix structure is sufficiently coarse to allow slip bands to crack the particles.
3. If 2 above is not obeyed, then the fracture strength varies as the inverse square root of the planar interparticle spacing.
4. Neither the yield nor the fracture strength varies directly with the volume fraction of carbide, but this parameter is important insofar as it affects the interparticle spacing.

Acknowledgements

The authors would like to express their appreciation to Jones and Laughlin Steel Co. for kindly supplying the materials used in this investigation and to the National Aeronautics and Space Administration for providing financial support under contract NASA NSG622.

REFERENCES

1. W. H. Bruckner, Weld Res. Supp., September, 1951, p 459--s.

2. A. S. Tetelman and A. J. McEvily, Jr., Fracture of Structural Materials, Wiley & Sons, New York, 1967.

3. C. J. McMahon, Jr. and M. Cohen, Acta Met., v. 13, 1965, p. 591.

4. D.P.H. Hasselman and R. M. Fulrath, J. of Amer. Ceramic Soc., v. 49, No. 2, February, 1966, p. 68.

5. G. T. Hahn and A. R. Rosenfield, Acta Met., v. 14, December, 1966, p. 1815.

6. T. L. Johnston, R. J. Stokes, and C. J. Li, Trans. AIME, v. 221, August, 1961, p. 792.

7. M. Ashby, Zeit. Metallkde., Bd. 55, 1964, H.1, p. 5.

8. G. T. Hahn and A. R. Rosenfield, Technical Report AFML - TR-65-409, Part II, March, 1967.

9. T. R. Wilshaw and P. L. Pratt, J. Mech. Phys. Solids, v. 14, 1966, p. 7.

10. J. F. Knott, Central Elec. Res. Lab. Rept. No. RD/L/R 1312, September, 1965.

11. J. R. Hendrickson, D. S. Wood, and D. S. Clark, Trans. ASM, v. 50, 1958, p. 656.

12. C. T. Liu, Tech. Rept., No. 23, Div. of Engineering, Brown University, Providence, R.I., August, 1967.

13. E. Orowan, Symposium on Strength of Metals, Inst. Met., 1948, p. 451.

14. G. Mima, Tech. Repts., Osaka University, v. 13, 1963, p. 123.

15. A. M. Turkalo, Trans. ASM, v. 54, 1961, p. 344.

16. J. D. Embury, A. S. Keh, and R. M. Fisher, Trans. AIME, v. 236, September, 1966, p. 1252.

17. J. R. Low, Jr., "The Fracture of Metals", Prog. in Mat. Sci., v. 12, No. 1, 1963.

18. N. J. Petch, JISI, May, 1953, p. 25.

19. R. A. Wullaert, PhD thesis, Stanford University, 1968.

20. T. R. Wilshaw, C. A. Rau, and A. S. Tetelman, Stanford University Report, SU-DMS, No. 67-9, March, 1967.

21. A. H. Cottrell, Trans. AIME, April, 1958, p. 192.

TABLE II

Steel	Tempering Temperature Deg. Cent.	λ_p Mean Free Particle Spacing, Microns	$(D_s - \bar{d})$ Free Inter-Particle Spacing, Microns	$d_{max.}$ Maximum Observed Particle Size, microns	σ_Y, Lower Yield Stress, (23C), Ksi	σ_f^*, Cleavage Fracture Stress, Ksi	$T_{D(N)}$ Nil Ductility Temperature Deg. Cent.
18MS	625	2.12	0.324	0.385	58.5	277.0	-162
18MS	500	0.975	0.149	0.20	79.0	340.0	-178
44	712	4.62	1.02	1.48	41.0	237.6	-125
44	550	2.0	0.44	0.98	65.5	268.0	-125
44M	700	3.62	0.80	1.33	60.5	229.0	-145
44M	590	1.32	0.29	0.43	77.5	309.6	-160
44M	500	0.75	0.17	0.38	98.75	359.0	-175
44MS	700	3.86	0.84	1.10	57.5	257.2	-150
44MS	500	--	--	0.40	97.5	327.0	-150
60	715	12.38	2.99	5.13	32.0	159.0	-71
60	540	3.70	0.89	1.01	67.0	264.0	-88
73	695	8.04	2.07	3.17	40.0	181.0	-72
73	572	3.27	0.84	1.45	60.5	235.0	-75
81M	690	3.45	0.92	1.38	59.5	261.6	-120
81M	600	1.65	0.44	0.89	77.5	296.5	-130
81M	505	0.50	0.13	0.55	112.0	353.0	-100
81M*	700-Q-450	0.23	0.07	1.78	~ 145.0	~ 375.0	~ -150

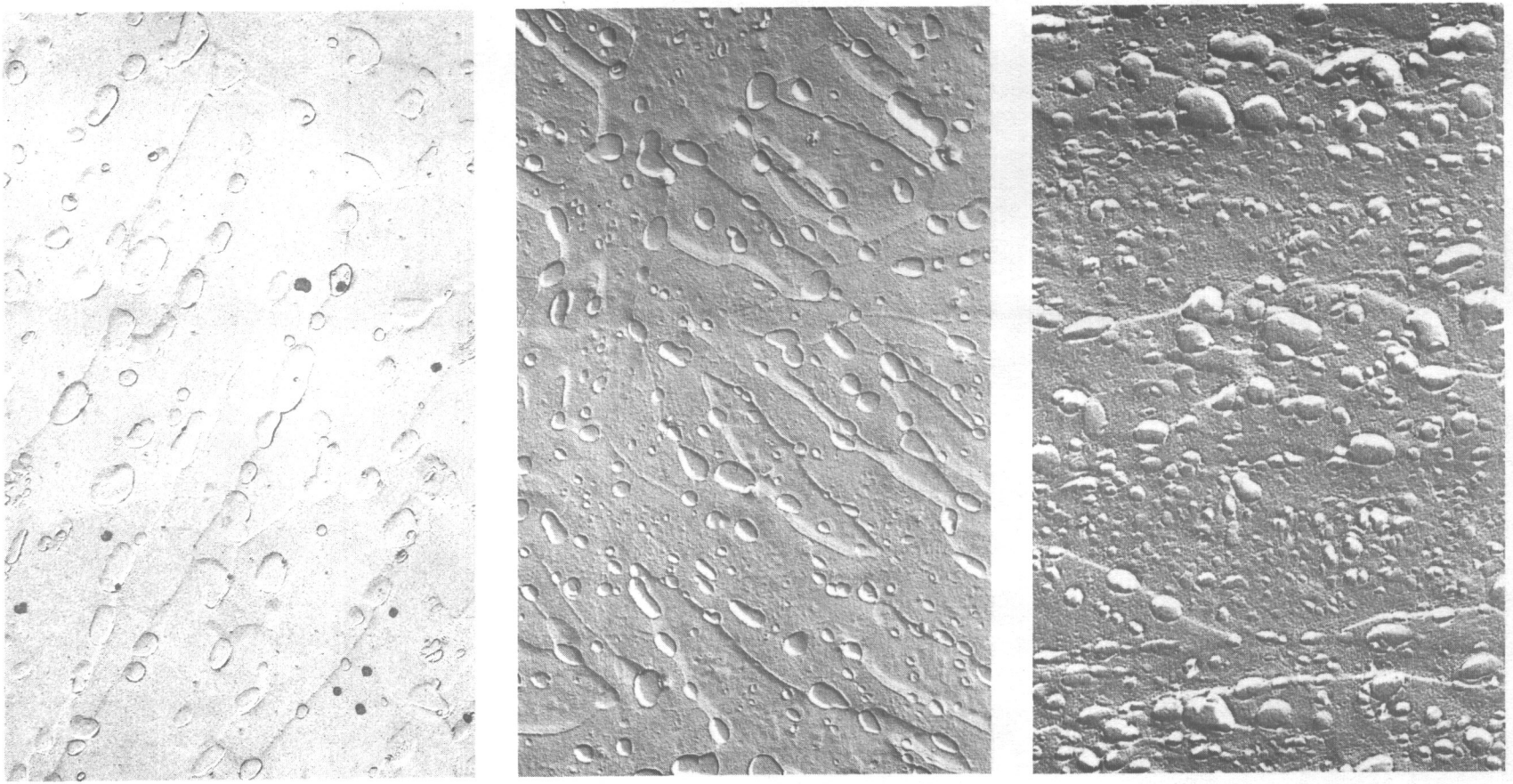

(a) (b) (c)

FIGURE 1. TYPICAL MICROSTRUCTURES OF QUENCHED AND TEMPERED STEELS. STEEL 44M TEMPERED AT (a) 700 C, (b) 590 C, and (c) 500 C, RESPECTIVELY. ELECTRO-ETCH IN PERCHLORIC-ACETIC ACID SOLUTION.

Figure 2. Steel 81M Double-Quenched-and-Tempered. Last Temper at 450C.

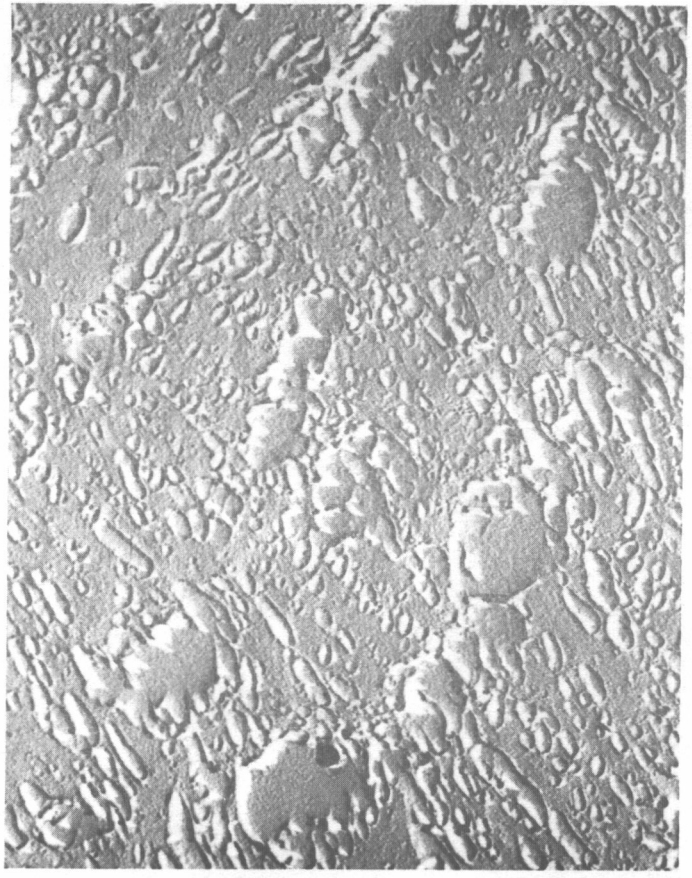

Figure 3. Microcrack in carbide occurring at low strain (<1%) in region of highest stress below a notch. Steel 60, 712C Temper.

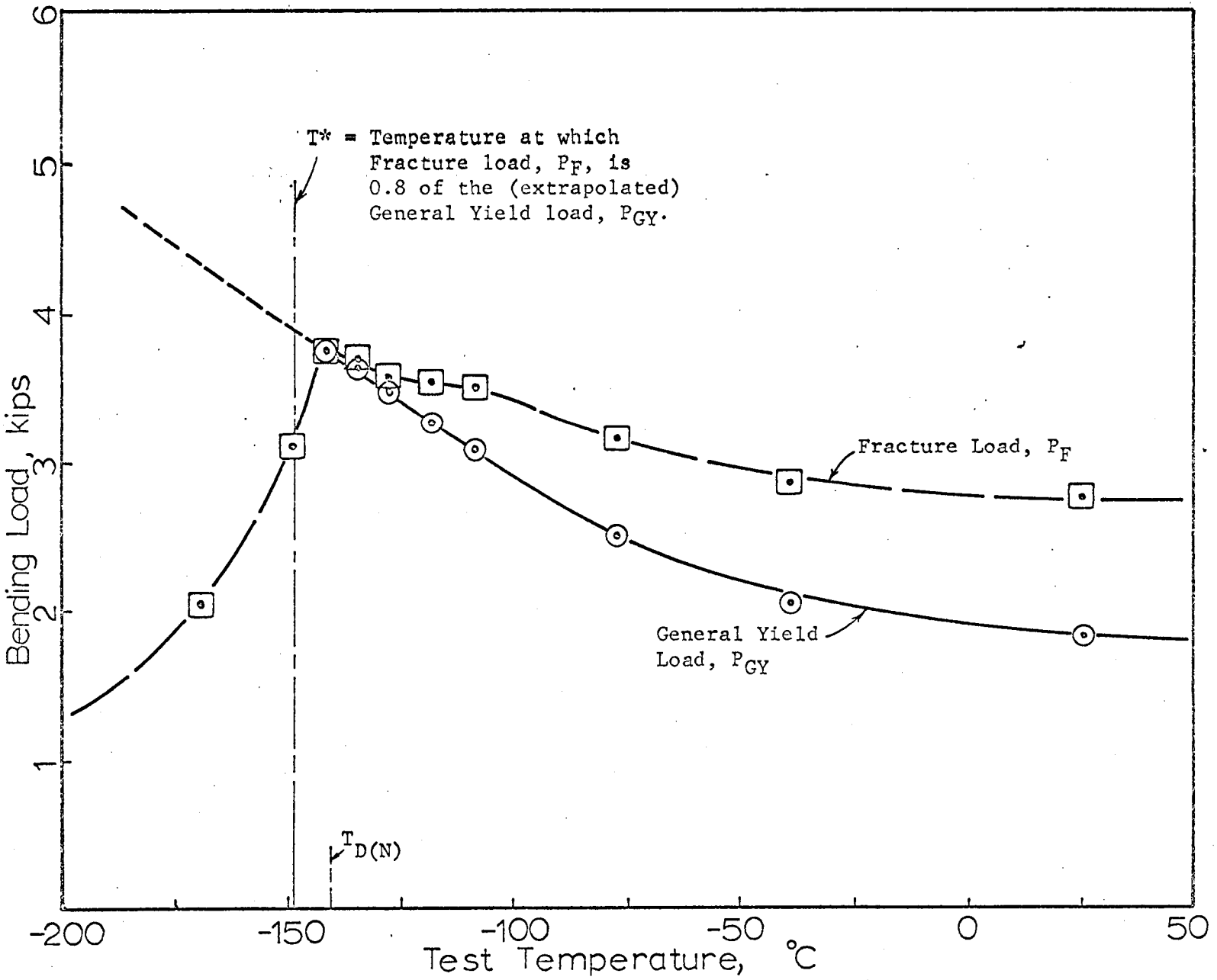

Figure 4. Typical curves of slow-bend Charpy general yield load and fracture load vs. test temperature (Steel 44M, 700C temper).

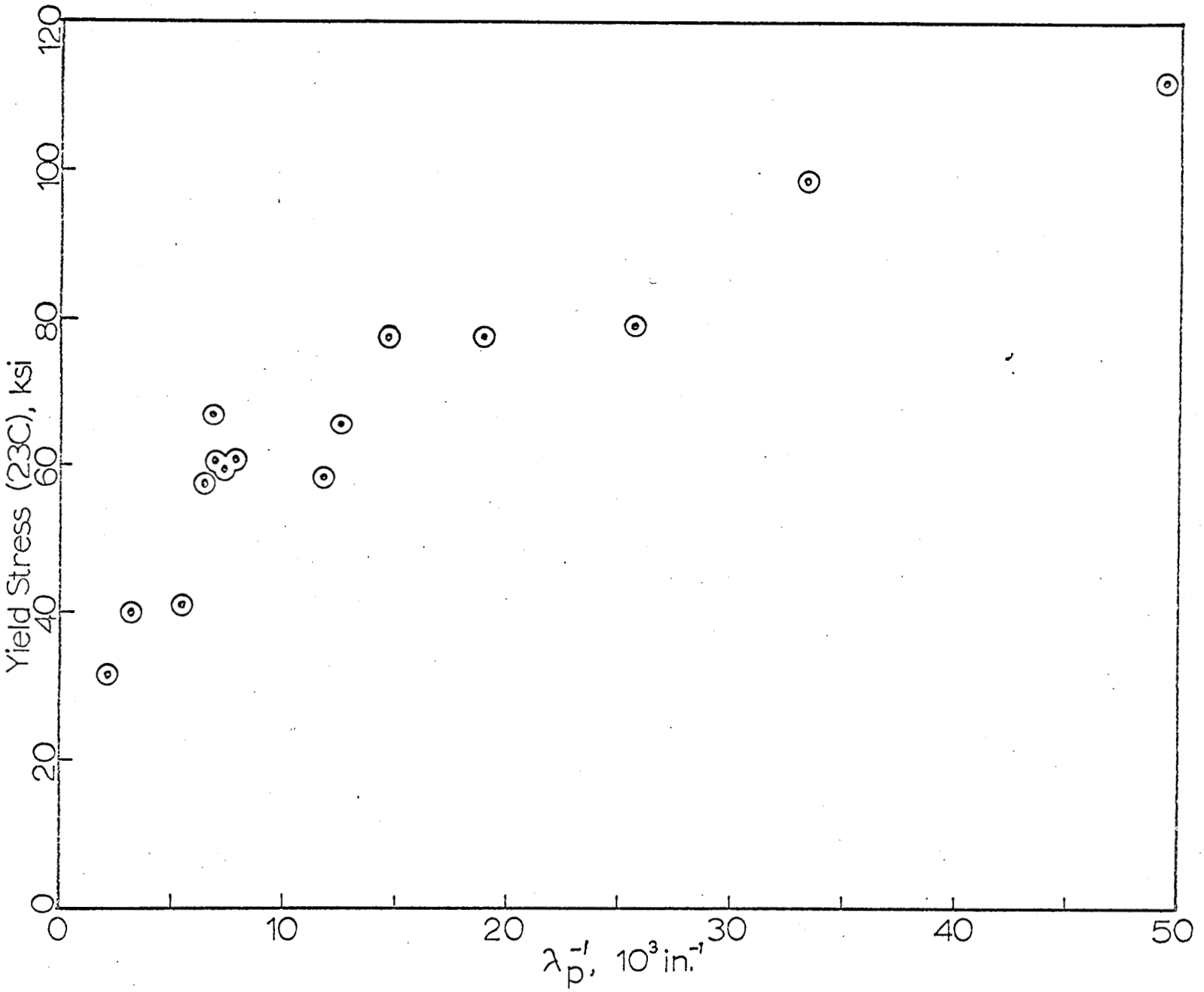

Figure 5. Room temperature yield stress plotted against the reciprocal of the mean free particle spacing.

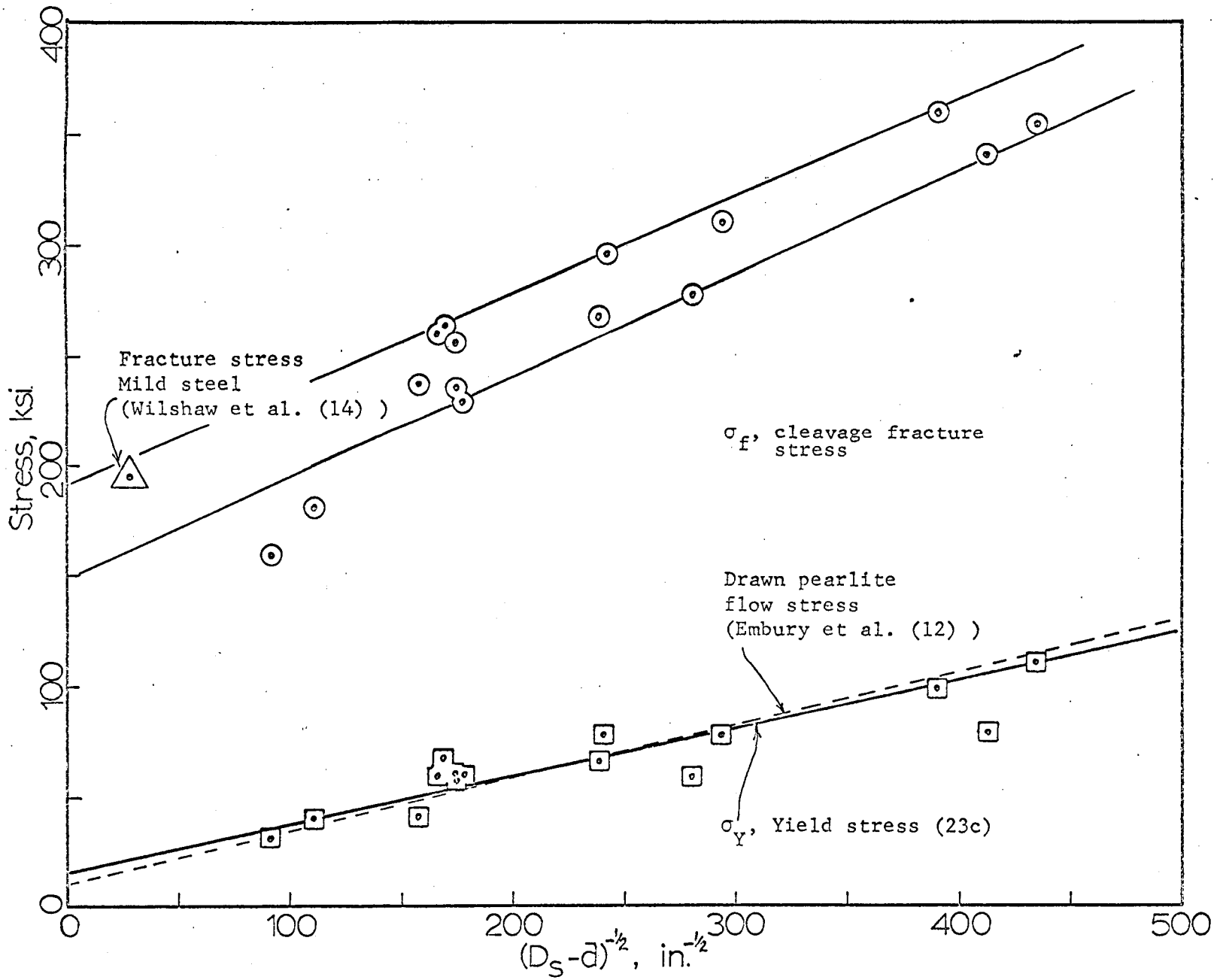

Figure 6. Room temperature yield stress and cleavage fracture stress vs. the reciprocal square root of the free interparticle spacing.

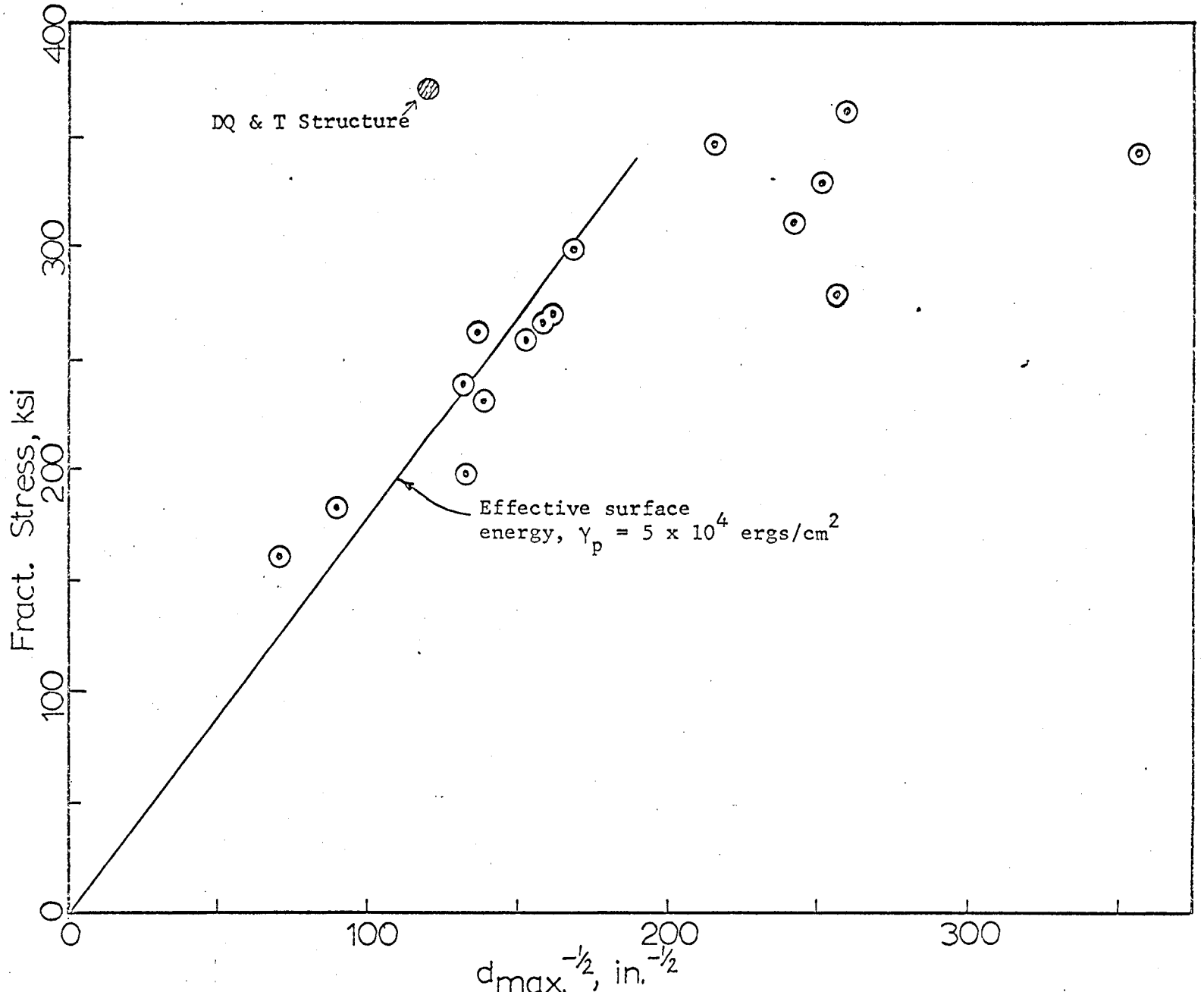

Figure 7. Cleavage fracture stress vs. the reciprocal square root of the diameter of the largest carbide particles in a structure.